Check for updates

JOURNAL OF Applied Polymer SCIENCE

Core-crosslinking as a pathway to develop inherently antibacterial polymeric micelles

Melike Seyma Kadayifci,[1] Damla Gokkaya,[1] Murat Topuzogullari,[1] Sevil Dincer Isoglu,[2] Tugba Atabey,[3] Tulin Arasoglu,[3] Mehmet Murat Ozmen[1]

[1]Department of Bioengineering, Yildiz Technical University, 34220, Istanbul, Turkey

[2]Department of Bioengineering, Abdullah Gul University, 38080, Kayseri, Turkey

[3]Department of Molecular Biology and Genetics, Yildiz Technical University, 34220, Istanbul, Turkey

Correspondence to: M. M. Ozmen (E-mail: ozmenm@yildiz.edu.tr)

ABSTRACT: Positively charged polymeric materials have been an alternative to combat bacteria as they exhibit inherently antibacterial potency via bacteria membrane disruption. In this study, we report facile preparation of positively charged core-crosslinked polymeric micelles with inherent antibacterial properties. Spherical micelles were prepared by self-assembling of poly(4-vinylpyridine)-*b*-(oligoethylene glycol methyl ether methacrylate) copolymer in aqueous solution. Herein, quaternization reaction was utilized for the first time to core crosslink the micelles through the pyridine rings utilizing their hydrophobic core and thus resulting positively charged nanostructures. Dynamic light scattering (DLS) results identified that the micelles have an average hydrodynamic diameter of 114 nm with a polydispersity index ranging between 0.105 and 0.114. The electrophoretic light scattering (ELS) measurements demonstrated that the micelles have zeta potential values ranging from +38 to +63 mV. It was evident from both ELS and DLS results that the micelles in solution exhibit long-term stability as the samples were able to maintain their size and charge even after a year of storage. Further, the micelles exhibited inherently antibacterial activity against *Escherichia coli* and furthermore, this antibacterial efficacy was sustained over a period of 1 year. These stable core-crosslinked micelles are proposed to have great potential as antibacterial materials for long-term applications. © 2019 Wiley Periodicals, Inc. J. Appl. Polym. Sci. **2020**, *137*, 48393.

KEYWORDS: bioengineering; copolymers; crosslinking; micelles; self-assembly

Received 26 April 2019; accepted 24 July 2019

DOI: 10.1002/app.48393

INTRODUCTION

Bacterial infections are a growing global problem that cause serious diseases all over the world and have become more challenging to treat due to the increased number of antibiotic resistant species.[1] The number of new antibiotics which have been developed and approved have been decreasing steadily in the last decades.[2] Therefore, it is highly necessary to develop novel antibacterial materials that have different bacteria killing mechanisms other than those of conventional antibiotics. Inherently, antibacterial polymeric materials have been of great interest in the prevention and/or treatment of bacterial diseases due to their versatility, biocompatibility, and nonimmunogenicity.[3,4] Cationic group containing polymers are the most widely known type of inherently antibacterial polymers previously used in many studies as either homopolymers or copolymers consisting of miscellaneous monomers.[5] These polymers display significant antibacterial activity potential after physical contact with the bacteria.[6,7] Principally, this occurs via the polycationic-rich surface of cationic polymers causing membrane disruption of the bacteria.[8]

Poly(4-vinylpyridine) (PVP) has been extensively studied to prepare polycations, as it is capable of gaining positive charge through quaternization of pendant pyridine rings. The quaternization of pyridine ring of PVP is an effective way of modifying the polymer structure to obtain side chains with different functional groups,[9] graft polymers,[10] or even gels.[11] In the last decades, this quaternary ammonium group containing PVP (quaternized PVP) has been used in several studies for antibacterial purposes as a soluble polymer,[12] gel,[13] or coating.[14] Although polycations containing quaternary ammonium groups have proven to exhibit inherent antibacterial effect,[15] they may cause toxicity to human or animal cells.[16] To overcome this drawback, a biocompatible and hydrophilic comonomer can be included into the structure of the polycation to obtain copolymer with reduced toxicity while retaining antibacterial activity. Youngblood *et al.* investigated such random copolymers of quaternized PVP with biocompatible oligoethylene glycol methyl ether methacrylate (OEGMA) monomer and successfully produced hemocompatible antibacterial copolymers.[12,17,18]

Additional Supporting Information may be found in the online version of this article.

© 2019 Wiley Periodicals, Inc.

Polymeric micelles bearing cationic groups have attracted interest in antibacterial applications as they exhibit increased antibacterial efficacy due to their high charge density and increased surface area.[19] However, since the micelles are self-assembled through noncovalent interactions, they can dissociate when exposed to environmental changes[20] such as dilution, temperature, and pH changes, and hence, this can lead to significant deterioration of their biological performance.[21] This lack of stability limits their long-term antibacterial effectiveness and breadth of applications.[22] Therefore, crosslinking is an efficient way to stabilize the micelles to prevent their dissociation into unimers.[23] To date, although a series of covalent bonds and reactions have been applied to micelle crosslinking including disulfide bonds,[24] thiol–ene reaction,[25] amide bond,[26] and so forth, as far as we know, quaternization reaction has not yet been used for crosslinking of any micelle. Thereby, quaternization can be considered as a facile alternative approach to concurrently achieve both crosslinking and positively charging of the micelles.

Recently, we have synthesized an amphiphilic block copolymer of PVP-*b*-poly(OEGMA) (POEGMA) for drug delivery and gene therapy purposes.[27,28] Herein, we prepared positively charged core-crosslinked micelles of the PVP-*b*-POEGMA copolymer by quaternization reaction. As these micelles would contain positively charged quaternary ammonium groups, we hypothesized that they are highly likely to exhibit inherent antibacterial activity. To achieve this, pyridine rings of the core forming PVP block were quaternized with bifunctional 1,6-dibromohexane (DBH) to form covalent crosslinks between polymer chains. The quaternization reaction resulted in the formation of a micelle structure with a positively charged PVP core within a hydrophilic shell of POEGMA blocks. To the best of our knowledge, this study represents the first polymeric micelle core-crosslinked via quaternization reaction. Moreover, as far as we are aware, we propose the first example of a core-crosslinked micelle with inherent antibacterial efficacy. As will be seen below, the obtained micelles show inherent antibacterial effect against *Escherichia coli* after overnight incubation, and thus can be used for antibacterial applications.

EXPERIMENTAL

Materials

OEGMA (M_n = 475 g mol^{-1}, Sigma-Aldrich, Istanbul, Turkey); 4-vinylpyridine (4VP, Sigma-Aldrich); azobisisobutyronitrile (AIBN, Sigma-Aldrich); DBH (Sigma-Aldrich); dichloromethane (Sigma-Aldrich); acetic acid (Sigma-Aldrich); 4-cyano-4-(phenylcarbonothioylthio)pentanoic acid (CTA, Strem Inc.); *N*,*N*-dimethylformamide (DMF, Carlo Erba); NaCl (Carlo Erba); and diethyl ether (Merck) were used as received. Ultrapure water was obtained from the Millipore Milli-Q water purification system. Mueller Hilton Broth/Agar media (Oxoid) was used for the antibacterial tests.

Synthesis of PVP-*b*-POEGMA Amphiphilic Block Copolymer via Reversible Addition–Fragmentation Chain Transfer Polymerization

PVP-*b*-POEGMA amphiphilic block copolymer was synthesized as described previously.[27] Briefly, OEGMA was polymerized with $[M]_0/[CTA]_0/[I]_0$ = 75/1/0.2 ratio. AIBN and CTA were used as the initiator and the reversible addition–fragmentation chain transfer (RAFT) agent, respectively. OEGMA was dissolved in DMF with the initial concentration of 0.5 M and CTA was added to this solution. The solution was purged with N_2 gas and heated to 70 °C. AIBN solution was added to initiate the polymerization of OEGMA. The reaction proceeded for 2 h and POEGMA was precipitated using cold diethyl ether. POEGMA was used as macroCTA to further mediate the RAFT polymerization. PVP block was extended from this macroCTA using the $[M]_0/[CTA]_0/[I]_0$ = 200/1/0.5 ratio. POEGMA was dissolved in DMF and 4VP was added to the solution. The mixture was exposed to N_2 gas and heated to 70 °C. The polymerization of 4VP was initiated by addition of AIBN solution. After 24 h, PVP-*b*-POEGMA copolymer was precipitated with cold diethyl ether and dried in vacuum incubator overnight at 50 °C. The conversions for POEGMA and PVP blocks were gravimetrically measured as 20 and 45%, respectively.

Preparation of Core-Crosslinked PVP-*b*-POEGMA Micelles through Quaternization

A total of 8 mg of PVP-*b*-POEGMA copolymer was dissolved in 1 mL of water and the crosslinker DBH was added to this solution. While the polymer concentration was kept constant, the DBH concentrations were varied based on the ratio of mole numbers of DBH (n_{DBH}) and 4VP units in the copolymer chain (n_{4VP}). As such, three micelles having molar ratios of n_{DBH}/n_{4VP} = 0.4, 0.25, and 0.1 were prepared and designated as M1, M2, and M3, respectively. Mixtures were vigorously stirred at room temperature for 30 min. Then, the temperature of the solutions was increased to 70 °C for the quaternization reaction. After 24 h of reaction, the mixtures were dialyzed against ultrapure water to remove any impurities. Finally, the obtained micelle solutions and their freeze-dried powders were kept at 4 °C until further use. The characterization of the micelle solutions were carried out at 25 °C and pH 7.

Characterization Techniques

The chemical structure of the PVP-*b*-POEGMA block copolymer was characterized with nuclear magnetic resonance (^{1}H-NMR) spectroscopy using Bruker AVANCE III 500 MHz NMR instrument. Gel permeation chromatography (GPC) analysis of the copolymer was carried out by Viscotek TDA302 instrument having refractive index and light scattering detectors (see Supporting Information for experimental details). Quaternization of micelles were determined using Fourier transform infrared (FTIR) spectra acquired from Shimadzu IR-Prestige 21 FTIR spectrophotometer with an attenuated total reflection apparatus. The hydrodynamic diameters (Dh), size distributions, and zeta potentials of micelles were measured by Malvern Zetasizer NanoZS dynamic light scattering (DLS) and electrophoretic light scattering (ELS) spectrometer.

The topography of the micelles was examined by scanning electron microscope (SEM) (Zeiss EVO LS 10). Samples were prepared by adding a drop of micelle solution on an SEM stub followed by drying of this solution in oven at 60 °C. Then, after, the samples were sputter coated by gold–palladium prior to the measurements. Using the same sample preparation route, Field Emission Gun Environmental SEM (FEI QUANTA 450 FEG

ESEM) was also used to investigate the micelles at much higher magnifications.

Antibacterial Assays

The antibacterial activity of micelles was evaluated by quantitative and qualitative analysis against *E. coli* (ATCC number: 25922) and *Staphylococcus aureus* (ATCC number: 25923). Disk and agar well diffusion methods were chosen as qualitative methods to assess the antibacterial activity of the micelles. Disk diffusion study was carried out based on the EUCAST standard.[29] Stock solutions of the micelles were prepared (2 mg mL^{-1}) and loaded over sterile blank disks. These disks were placed on agar plates containing the inoculated bacteria.

The agar well diffusion test was carried out as described before.[30] The stock solutions (2 mg mL^{-1}) prepared for the disk diffusion method were also used and added to the wells as 100 μL. These two qualitative methods were evaluated according to the appearance of inhibition zone around the disks and wells.

Broth microdilution method was chosen as the quantitative method to screen the *in vitro* antibacterial activity of micelles. Broth microdilution was performed in accordance with the CLSI standard.[31] To determine the minimum inhibitory concentration (MIC) of the micelles, serial dilutions of the micelle stock solutions were prepared in liquid growth medium using a 96-well plate. The bacterial culture medium (10^6 cfu mL^{-1}) was added into each well and the final volume of the wells was adjusted to 300 μL. These culture plates were incubated at 37 °C for 24 h. While the negative control wells were only broth and bacteria without any agent, the blank control wells were only broth without bacteria. The positive control wells were both vancomycin antibiotic solutions (4 mg L^{-1}) and bacteria. MIC values were determined by both spectrophotometric measurements (OD600 nm) and standard plate counting method.

RESULTS AND DISCUSSION

The aim of this study was to utilize quaternization reaction to form positively charged core-crosslinked micelles and furthermore, to investigate their antibacterial efficacy. PVP-*b*-POEGMA block copolymer was used as the unimer of the micelles in which POEGMA is the hydrophilic block, and PVP as the core-forming hydrophobic block. This type of copolymer including a PVP core and PEG side chains has a coil-brush-like structure that provides more PEG chains per PVP, thus enhancing the copolymer's solubility and biocompatibility. By quaternization of PVP segments with a bifunctional alkylating agent, a positively charged and crosslinked core was formed surrounded by a POEGMA shell.

A two-step RAFT polymerization resulted in PVP-*b*-POEGMA copolymer to be used in the formation of micelles. GPC chromatograms of POEGMA and PVP-*b*-POEGMA displayed that the POEGMA (M_n = 15 kg mol^{-1}) is eluted later than the PVP-*b*-POEGMA block copolymer (M_n = 29 kg mol^{-1}) (Figure S1). Moreover, the GPC analysis indicated a controlled polymerization with a low polydispersity as polydispersity index (PDI) values were 1.09 and 1.33 for POEGMA and the block copolymer, respectively. Chemical structure of the PVP-*b*-POEGMA copolymer was characterized using ^{1}H-NMR spectroscopy. The protons of OEGMA and 4VP units of the block copolymer were obvious in the ^{1}H-NMR spectrum of the copolymer in which the protons of pyridine rings are at 8.2 and 6.6 ppm and peaks at 4.0, 3.5, and 3.3 ppm belong to OEGMA (Figure S2). Hence, both the GPC chromatograms and NMR spectrum revealed the successful synthesis of the PVP-*b*-POEGMA block copolymer.

In order to obtain the micelles, the prepared PVP-*b*-POEGMA copolymer was dissolved in water. Since the block copolymer has an amphiphilic structure, micelles were formed spontaneously in water due to the hydrophobic effect. Thereafter, crosslinking in the micelle structure was carried out to stabilize the polymeric micelles. Here, we used the bifunctional quaternization agent DBH for crosslinking of micelles through the pyridine rings within the core using a two-step procedure (Scheme 1). In the first step, micelles of PVP-*b*-POEGMA copolymers were formed spontaneously at room temperature by hydrophobic effect caused by the hydrophobicity of PVP block and DBH molecules. In the second step, these micelle solutions were heated to 70 °C to facilitate the quaternization reaction, evident by the clarification of the solutions which indicates the successful incorporation of DBH into the hydrophobic core of the micelle. Here, heating the micelle solution enabled the alkylation of tertiary amines in pyridine rings with bifunctional DBH to form positively charged quaternized pyridine rings in the core of the micelle. Consequently, a novel core-crosslinked micelle that has a positively charged core and a nonionic, biocompatible, hydrophilic shell was obtained.

The structure of the dried core-crosslinked micelles was investigated by FTIR spectrometry. FTIR is a quite definitive method for determination of the quaternization of pyridine rings as it identifies bands at 1600 and 1640 cm^{-1} characteristically belonging to pyridine and quaternized pyridine rings, respectively.[32] As is shown in Figure 1, all micelles have bands at 1600 cm^{-1} (C═C bending) indicating pyridine rings and 1640 cm^{-1} (C═C stretching) belonging to quaternized pyridine rings. Also, the band at 1720 cm^{-1} (C═O stretching) depicts the carbonyl group of the POEGMA block of the copolymer. For comparison, the FTIR spectrum of nonquaternized PVP-*b*-POEGMA copolymer which was not subjected to quaternization reaction is also shown in Figure 1. In the copolymer spectrum, the peak at 1640 cm^{-1} was not observed due to the absence of quaternized pyridine rings.

To further confirm the formation of micelles, physicochemical properties such as size, charge, and shape of the samples were investigated. Figure 2 shows the hydrodynamic size distributions of micelles measured via DLS in which the micelles exhibit unimodal size distributions. z-Average hydrodynamic diameter values of the micelles were 116, 113, and 113 nm for M1, M2, and M3, respectively. Moreover, the polydispersity of micelles ranging between 0.105 and 0.114 also proves that secondary aggregations were not occurred during micelle formation because of the hydrophobic chains or covalent crosslinks.

DLS measurements also enable investigation of the stability of the micelles by determining the critical micelle concentration (CMC) at which the micelles dissociate to unimers.[33] Light scattering intensity of the unimeric polymers increases significantly

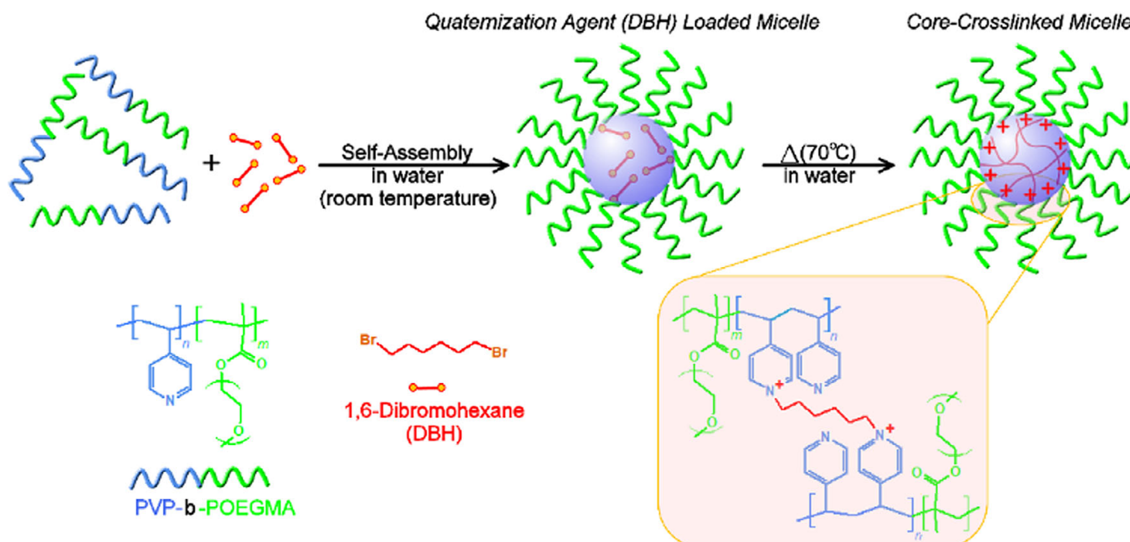

Scheme 1. Quaternization crosslinking of PVP-*b*-POEGMA copolymer in aqueous solution yielding positively charged core-crosslinked micelles. [Color figure can be viewed at wileyonlinelibrary.com]

after formation of micelles since they are much larger than unimers. Therefore, the CMC of micelles can be determined by measuring the light scattering intensity of micelle solution at various concentrations. Thus, we conducted DLS measurements to confirm the stability of the micelles upon dilution of the micelle solution. Figure 3 shows the light scattering intensity of the Micelle M3 as a function of the micelle concentration. In Figure 3, light scattering intensity linearly increases with the concentration of micelle and the variation in the slope of the curve is not observed, indicating intact micelles and no dissociation of the micelles. Furthermore, when measured by DLS, the hydrodynamic size of unimeric polymers is significantly smaller than the micelles. It is noteworthy that size of the micelles is between 100 and 160 nm (Figure 3) and reduction in size is not observed upon dilution of micelle solutions. Hence, it is evident that the quaternization core crosslinking of micelles maintains the stability of micelles even at very low concentrations preventing dissociation of micelles into unimers.

The morphologies of the dried micelles were analyzed by SEM. As illustrated in Figure 4, the spherical morphologies of the dried micelles were confirmed by SEM images and the diameter of the spherical micelles were measured as ~120 nm for M1, M2, and M3 in accordance with the hydrodynamic diameters acquired by DLS, as aforementioned. Further, the insets in Figure 4 display the corresponding FEG ESEM images of single micelle at higher magnifications. The diameters of single micelle shown as inset in Figure 4 were also measured in the range of 110 and 130 nm. As a consequence, the hydrodynamic size distributions given above

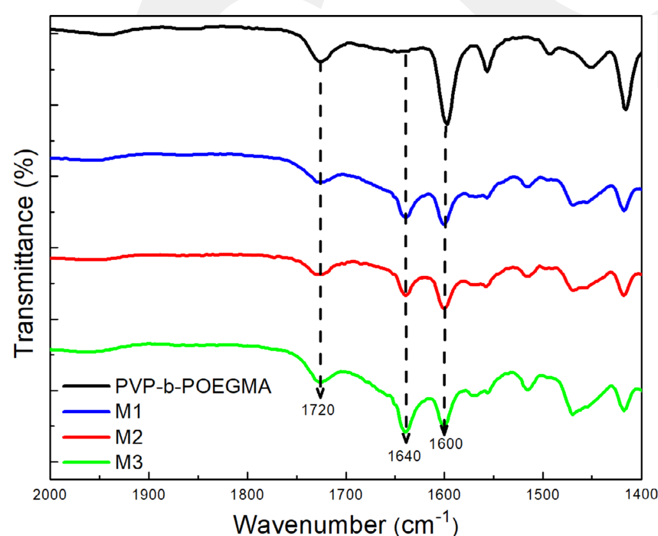

Figure 1. FTIR spectra of the PVP-*b*-POEGMA micelles after quaternization of pyridine rings in the core of the micelles and nonquaternized PVP-*b*-POEGMA copolymer. [Color figure can be viewed at wileyonlinelibrary.com]

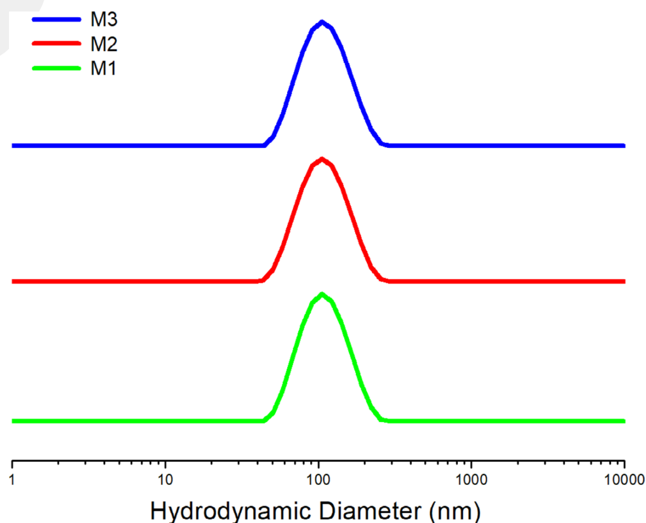

Figure 2. Intensity-based hydrodynamic size distributions of Micelles M1, M2, and M3 acquired from DLS measurements. [Color figure can be viewed at wileyonlinelibrary.com]

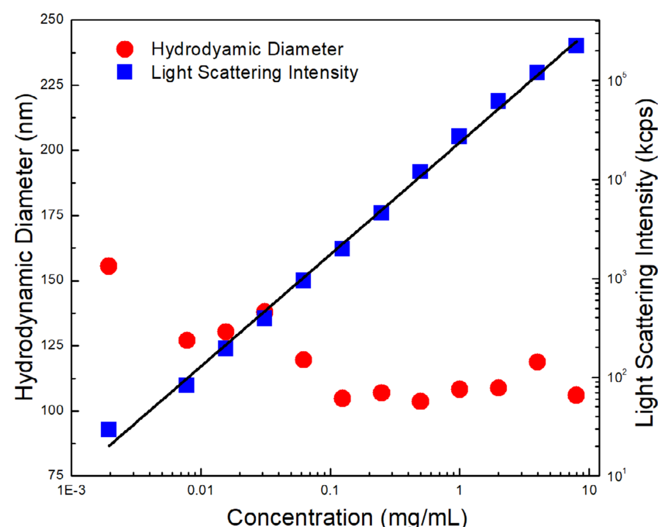

Figure 3. Light scattering intensity and hydrodynamic diameter of M3 as a function of copolymer concentration. [Color figure can be viewed at wileyonlinelibrary.com]

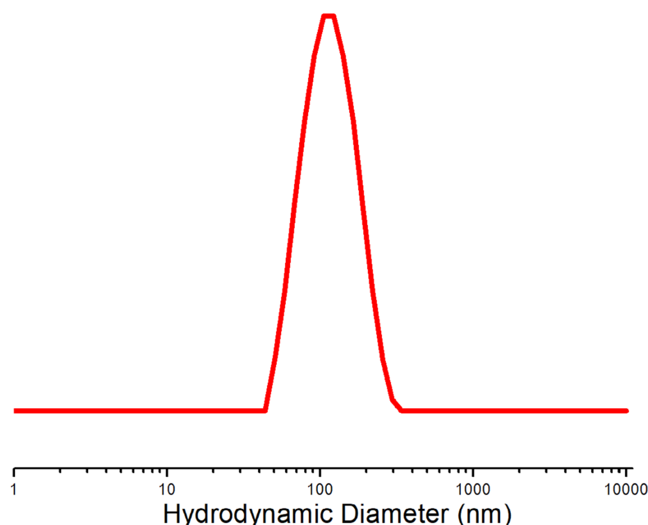

Figure 5. Intensity-based hydrodynamic size distribution of Micelle M3 solution stored for 1 year. [Color figure can be viewed at wileyonlinelibrary.com]

and the SEM images reveal the formation of monodisperse and nanosized spherical micelles with equivalent micelle diameters.

Quaternization reaction transforms the pyridine rings of PVP block to quaternary pyridinium ions, which are positively charged at all pH values. The surface charge of cationic structures is an important factor that affects their antibacterial efficacy. Therefore, zeta potential measurements were carried out to determine the positive charge on the surfaces of micelles. ELS measurements were conducted to determine the zeta potentials of micelles. Zeta potential values of +63, +51, and +38 mV were acquired for M1, M2, and M3, respectively. The increase in zeta potential values with the quantity of crosslinker indicates that higher amount of DBH reacts with more pyridine rings. Our results were in accordance with previously reported results as it is known that increasing the amount of quaternization agent increases the zeta potentials of the polycation.[34]

The time-dependent stability of antibacterial agents is important when long-term antibacterial applications are considered.[35,36] To investigate the long-term stability of the obtained micelles, the solutions of samples were stored for 1 year at 4 °C. Figure 5 shows the results of the hydrodynamic size distribution measurements of Micelle M3 which was stored for 1 year. As Figure 5 reveals, M3 has a unimodal distribution with z-average diameter of 110 nm and zeta potential of +38.8 mV after 1 year of storage. Thus, comparison with the initial size and zeta potential results provides strong evidence that the core-crosslinked micelles have retained their size and positive charges stable for 1 year. Moreover, it is important to note that there is no agglomeration of the micelles even after 1 year of storage in aqueous solution.

The antibacterial activity of the micelles was evaluated by three different methods including broth microdilution, disk diffusion, and agar well diffusion where *E. coli* (ATCC number: 25922) and *S. aureus* (ATCC number: 25923) were used as Gram-negative and Gram-positive bacteria models, respectively. According to the results of the agar well diffusion and disk diffusion methods, the samples did not exhibit a considerable growth inhibition zone at the tested concentrations (data not shown). This indicates that the micelles did not diffuse neither in disk diffusion nor in well diffusion systems. We envisage that the size or charge of the

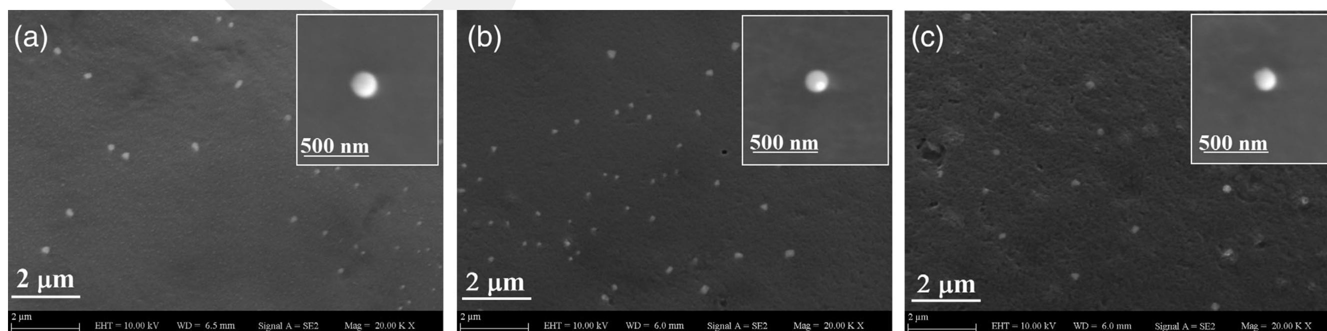

Figure 4. SEM images of dried micelles M1 (a), M2 (b), and, M3 (c) at 20,000× magnification. The insets show 12,0000× magnified images of each micelle acquired by FEG ESEM.

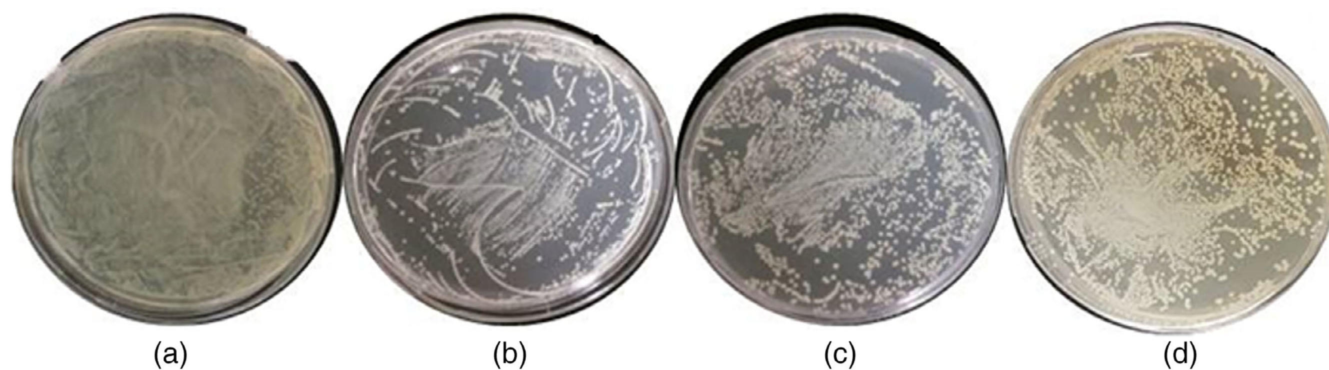

Figure 6. The twofold diluted Petri images of standard plate count method in broth microdilution assay (a) *E. coli* control group, (b) M1, (c) M2, and (d) M3, respectively. [Color figure can be viewed at wileyonlinelibrary.com]

micelles prevent their diffusion inside the agar medium. While the size of the micelles may have prevented penetration through the gaps in agar gel, the positively charged micelles may have electrostatically interacted with negatively charged agar components, such as sulfate groups of agaropectin. Indeed, it was reported that even small numbers of countercharged regions in gel structure can have a strong trapping effect for charged particles via electrostatic attraction.[37]

MIC values were determined by both spectrophotometric measurements at 600 nm and standard plate count method to achieve more reliable results. While any MIC value was not detected at the concentrations tested for *S. aureus*, the M1, M2, and M3 micelles exhibited antibacterial activity against *E. coli* given that the samples showed inhibitory activity at the highest concentration level with MIC values of 0.6 mg mL^{-1}. The high MIC values of the micelles compared to the relevant state-of-the-art nanomaterials reported in the literature[38] can be attributed to the fact that the positive charge of the obtained nanostructures are located in the core of the micelles, thus diminishing their direct contact with the bacteria. Based on the MIC values observed, although it may appear that the antibacterial efficacy is limited, these values as a proof of concept support our hypothesis that core-crosslinked micelles with positively charged core have the potential for antibacterial applications.

Besides, MIC values revealed that different zeta potential values of M1, M2, and M3 did not influence their antibacterial activities. On the contrary, standard plate count technique results indicate that the charge of the micelle affects the antibacterial efficacy of the samples. As shown in Figure 6, dilution Petri images using standard plate count technique exhibits that colony number is significantly reduced depending on the zeta potential values of the micelles. For instance, in Figure 6(b), it is clear that Sample M1 having the highest zeta potential of +61 mV, has the lowest colony number. Thus, it can be deduced that although the positive charges are hidden in the core of the micelles, higher positive charge in the core directly results in an enhanced antibacterial efficacy. This is advantageous as it enables to tailor the antibacterial performance of the micelles by varying the amount of the positive charges.

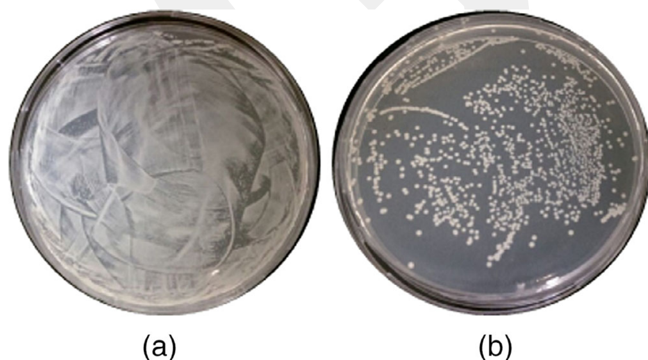

Figure 7. The twofold diluted Petri images of standard plate count technique in broth microdilution method. (a) *E. coli* control group and (b) the M3 micelle solution after 1 year of storage at 4 °C. [Color figure can be viewed at wileyonlinelibrary.com]

The difference in antibacterial activity of micelles against Gram-positive (*S. aureus*) and Gram-negative (*E. coli*) can be correlated with the differences in the cell wall structures of these bacteria. Recently, it was shown that the presence of a higher number of negative charges on the cell wall of the Gram-negative bacteria (*E. coli*) causes stronger electrostatic interactions with the counter charged micelles.[39] It was reported that *E. coli* and *S. aureus* have surface charges of −18.2 mV and −7.13 mV, respectively, indicating that *S. aureus* bacteria were significantly less negatively charged than *E. coli*. Accordingly, the highly positively charged Micelle M1 is likely to induce stronger interaction with the more negatively charged *E. coli*. Therefore, Sample M1 exhibited more efficient antibacterial activity by reducing a higher number of live colonies via bacterial lysis. Our antibacterial activity results reveal a better antibacterial performance when compared with 10,000 μg mL^{-1} MIC values against *E. coli* reported in the previous study where antibacterial crosslinked nanoparticles of vinylpyridine and ethylene glycol dimethacrylate were prepared.[40] This is because of the increased hydrophilicity of the micelles due to the POEGMA shell which enhances the solubility of the material, and thus improving the interaction with the bacterial membrane.

In addition, to investigate the long-term antibacterial efficacy of the micelles, broth microdilution assays were also conducted for the micelles stored as solutions for 1 year. As expected, the M3 micelle has shown similar antibacterial activity against *E. coli* (MIC value of 0.6 mg mL^{-1}) after 1 year storage given that its size, size distribution, and zeta potential values were also maintained. Furthermore, this long-term antibacterial stability was also investigated by standard plate count assay and the results are displayed in Figure 7. It is obvious in Figure 7 that the

micelle is still effective against *E. coli* after 1 year as the colony number is reduced as well.

CONCLUSIONS

Quaternization reaction has been successfully applied to the core crosslinking of PVP-*b*-POEGMA micelles resulting in novel, stable, and inherently antibacterial cationic polymeric materials. The stable micelles could maintain their size and charge over a year. Moreover, the antibacterial activity assays resulted in the inhibition of *E. coli* (selected Gram-negative model organism) bacterial growth which was also maintained after 1 year. Considering the long-term stability of micelles and the MIC values achieved from the antibacterial tests, these micelles are potential candidates for long-term antibacterial applications, that is, textile products or surface coatings. Finally, we envisage that our simple core-crosslinking strategy via quaternization can be a crucial pathway leading to the development of new positively charged inherently antibacterial polymeric micelles.

CONFLICT OF INTEREST

The authors declare no conflict of interest.

REFERENCES

1. Walker, T.; Dumadag, S.; Lee, C. J.; Lee, S. H.; Bender, J. M.; Cupo Abbott, J.; She, R. C. *J. Clin. Microbiol.* **2016**, *54*, 1789.
2. Ventola, C. L. *Pharm. Therap.* **2015**, *40*, 277.
3. Carmona-Ribeiro, A.; de Melo Carrasco, L. *Int. J. Mol. Sci.* **2013**, *14*, 9906.
4. Song, R.; Murphy, M.; Li, C.; Ting, K.; Soo, C.; Zheng, Z. *Drug Des. Devel. Ther.* **2018**, *12*, 3117.
5. Samal, S. K.; Dash, M.; Van Vlierberghe, S.; Kaplan, D. L.; Chiellini, E.; van Blitterswijk, C.; Moroni, L.; Dubruel, P. *Chem. Soc. Rev.* **2012**, *41*, 7147.
6. Kenawy, E.-R.; Abdel-Hay, F. I.; El-Shanshoury, A. E.-R. R.; El-Newehy, M. H. *J. Control. Release*. **1998**, *50*, 145.
7. Lu, G.; Wu, D.; Fu, R. *React. Funct. Polym.* **2007**, *67*, 355.
8. Shirbin, S. J.; Lam, S. J.; Chan, N. J.-A.; Ozmen, M. M.; Fu, Q.; O'Brien-Simpson, N.; Reynolds, E. C.; Qiao, G. G. *ACS Macro Lett.* **2016**, *5*, 552.
9. Bicak, N.; Gazi, M. *J. Macromol. Sci. Part A*. **2003**, *40*, 585.
10. Mansri, A.; Frère, Y.; Chovino, C.; Gramain, P. *Des. Monomers Polym.* **2000**, *3*, 55.
11. Zhou, X.; Nie, J.; Xu, J.; Du, B. *Colloid Polym. Sci.* **2015**, *293*, 2101.
12. Allison, B. C.; Applegate, B. M.; Youngblood, J. P. *Biomacromolecules*. **2007**, *8*, 2995.
13. Silan, C.; Akcali, A.; Otkun, M. T.; Ozbey, N.; Butun, S.; Ozay, O.; Sahiner, N. *Colloids Surf. B Biointerfaces*. **2012**, *89*, 248.
14. Cen, L.; Neoh, K. G.; Kang, E. T. *Langmuir*. **2003**, *19*, 10295.
15. Kenawy, E.-R.; Worley, S.; Broughton, R. *Biomacromolecules*. **2007**, *8*, 1359.
16. Xue, Y.; Xiao, H.; Zhang, Y. *Int. J. Mol. Sci.* **2015**, *16*, 3626.
17. Stratton, T. R.; Howarter, J. A.; Allison, B. C.; Applegate, B. M.; Youngblood, J. P. *Biomacromolecules*. **2010**, *11*, 1286.
18. Stratton, T. R.; Rickus, J. L.; Youngblood, J. P. *Biomacromolecules*. **2009**, *10*, 2550.
19. Lam, S. J.; Wong, E. H. H.; Boyer, C.; Qiao, G. G. *Prog. Polym. Sci.* **2018**, *76*, 40.
20. Owen, S. C.; Chan, D. P.; Shoichet, M. S. *Nano Today*. **2012**, *7*, 53.
21. Talelli, M.; Barz, M.; Rijcken, C. J. F.; Kiessling, F.; Hennink, W. E.; Lammers, T. *Nano Today*. **2015**, *10*, 93.
22. Huo, D.; He, J.; Li, H.; Yu, H.; Shi, T.; Feng, Y.; Zhou, Z.; Hu, Y. *Colloids Surf. B Biointerfaces*. **2014**, *117*, 29.
23. Isoglu, I. A.; Ozsoy, Y.; Dincer Isoglu, S. *Curr. Top. Med. Chem.* **2017**, *17*, 1469.
24. Matsumoto, S.; Christie, R. J.; Nishiyama, N.; Miyata, K.; Ishii, A.; Oba, M.; Koyama, H.; Yamasaki, Y.; Kataoka, K. *Biomacromolecules*. **2009**, *10*, 119.
25. Ma, J.; Bartels, J. W.; Li, Z.; Zhang, K.; Cheng, C.; Wooley, K. L. *Aus. J. Chem.* **2010**, *63*, 1159.
26. Wooley, K.; Remsen, E. *Chem. Commun.* **1998**, *13*, 1415.
27. Topuzogullari, M.; Bulmus, V.; Dalgakiran, E.; Dinçer, S. *Polymer*. **2014**, *55*, 525.
28. Topuzogullari, M.; Elalmis, Y. B.; Isoglu, S. D. *Macromol. Biosci.* **2017**, *17*, 1600263.
29. The European Committee on Antimicrobial Susceptibility Testing. Breakpoint tables for interpretation of MICs and zone diameters. Version 9.0, **2019**.
30. Arasoglu, T.; Derman, S.; Mansuroglu, B.; Yelkenci, G.; Kocyigit, B.; Gumus, B.; Acar, T.; Kocacaliskan, I. *J. Appl. Microbiol.* **2017**, *123*, 1407.
31. Methods for Dilution Antimicrobial Susceptibility Tests for Bacteria that Grow Aerobically; approved standard–9th ed. Broth Dilution Procedures (Macrodilution and Microdilution); Clinical & Laboratory Standards Institute, **2012**.
32. Panov, V. P.; Vorontsov, E. D.; Evdakov, V. P. *J. Appl. Spectrosc.* **1975**, *23*, 111.
33. Topel, Ö.; Çakır, B. A.; Budama, L.; Hoda, N. *J. Mol. Liq.* **2013**, *177*, 40.
34. Mao, Z.; Ma, L.; Jiang, Y.; Yan, M.; Gao, C.; Shen, J. *Macromol. Biosci.* **2007**, *7*, 855.
35. Korshed, P.; Li, L.; Ngo, D.-T.; Wang, T. *Nanomaterials*. **2018**, *8*, 218.
36. Yang, Z.; Hao, X.; Chen, S.; Ma, Z.; Wang, W.; Wang, C.; Yue, L.; Sun, H.; Shao, Q.; Murugadoss, V.; Guo, Z. *J. Colloid Interface Sci.* **2019**, *533*, 13.
37. Hansing, J.; Duke, J. R., III; Fryman, E. B.; DeRouchey, J. E.; Netz, R. R. *Nano Lett.* **2018**, *18*, 5248.
38. de Almeida, N. R.; Han, Y.; Perez, J.; Kirkpatrick, S.; Wang, Y.; Sheridan, M. C. *ACS Appl. Mater. Interfaces*. **2019**, *11*, 2790.
39. Arasoglu, T.; Derman, S.; Mansuroglu, B. *Nanotechnology*. **2015**, *27*, 025103.
40. Ozay, O.; Akcali, A.; Otkun, M. T.; Silan, C.; Aktas, N.; Sahiner, N. *Colloids Surf. B: Biointerfaces*. **2010**, *79*, 460.